BMSM

Bulletin of Materials Science & Metallurgy

Periodical Scientific Journal of UCTEA Chamber of Metallurgical and Materials Engineers

Volume 1, Issue 3, 2024, Pages 1-6 Received: 07 November 2024 Accepted: 25 December 2024

https://doi.org/10.70342/VFYD5509

Research Article

Effect of intensive milling on the structural characteristics of shale ore

Turan Uysal[a,*], Tufan Kıyak[b], Hikmet Sis[b], Murat Erdemoğlu[b]

[a]Gümüşhane University, Mining Engineering Department, Gümüşhane, Turkiye

[b]İnönü University, Mining Engineering Department, Malatya, Turkiye

*Corresponding author's email: turanuysal@gumushane.edu.tr

Abstract

This investigation examined the effect of intensive milling on the structural properties of shale ore with high Rare Earth Element (REE) content, which is unsuitable for aluminum production due to high silica and/or low aluminum. In this context, bauxite-related shale ore from the Karaman province in Türkiye was subjected to intensive milling under various conditions. Representative samples were collected from the deposit were first subjected to coarse crushing and milling processes, and then were excessively milled in a planetary ball mill under different conditions to ensure their mechanical activation. Changes occurred during milling were examined by XRD, TGA, BET and SEM analysis. The characterization results of intensively milled and unmilled samples showed that the intensive-milled samples were mechanically activated. As a result, the usability of mechanically activated shale for the recovery of Al and REEs from shale ore was evaluated.

Keywords

Shale; Rare earth element; Milling; Mechanical activation

1. Introduction

The mechanical activation of minerals increases the selective dissolution and solvent efficiencies during leaching, leading to an increase in the reaction rate [1]. This increase occurs as a result of an increase in the specific surface area and structural disorder [2], an increase in microstress [3], amorphization of mineral crystals [4], microtopographic changes [5], the formation of new phases more prone to dissolution [6], and a tendency for thermal reduction [7]. In the case of mechanical activation, the mineral behaves more actively during metallurgical processes such as calcination [8], roasting [9], or leaching [10], which reduces the temperature of the process or increases its speed.

In mechanically activated materials, the plastic deformation and irregularity of the crystal structure, that is, the formation of lattice distortion, lattice defects, and dislocation density, increase. Thus, the crystal structure becomes amorphous with intensive milling. In this case, displacement of the XRD diffraction peaks of the minerals was observed as broadening, shortening, or disappearance of the peaks.

Rare Earth Elements (REEs) are indispensable to modern materials and energy technologies. REEs are widely used in the production of many high-tech devices and equipment, such as electric/hybrid vehicles, wind turbines, solar panels, aircraft, and electronic devices, such as cell phones, computers, rechargeable batteries, and modern medical devices, such as MRI devices [11]. In particular, the demand for REEs (Nd, Pr, Tb, and Dy) used in magnet production is expected to increase, and the supply of these elements is expected to be problematic as of 2025. Therefore, countries have sought to produce REE from secondary geological sources such as ionic clays, red mud and bauxite-related shales with low U and Th content [12-13].

The Kızıldağ bauxite mineralization in Türkiye are situated within the Bolkar Mountain Bauxite Province. The protolith, or source rocks, of the Bolkar Mountain bauxite mineralization was identified as shale by Hanilçi [14]. Heavy REE

enrichment is characteristic of these deposits, and bauxite deposits, along with their source rocks and shales, contain significant concentrations of REEs that may serve as potential sources. Researchers [15-18] have investigated the formation of REE in bauxite-related deposits in the Bolkar mountain region and determined that clay minerals formed during the lateritic weathering process compensate for the lack of electrostatic charge on their outer edges with ions, such as Ca^{2+}, Na^{+}, and REE^{3-}. Consequently, REEs were enriched through adsorption on the outer surface of the clay. These REE-rich clays were subsequently formed by the addition of bauxite [2].

Mechanical activation, the mineral behaves more actively during metallurgical processes such as roasting [9] or leaching [10] which reduces the temperature of the process or increases its speed. In this context, Kızıldağ shale ore was intensively milled before the acidic leaching. The intensively milled ore was characterized using different characterization methods, and the effect of intensive milling was investigated.

2. Materials and Methods

In this study, shale ore was selected in a representative piece size from the mines that belong to the Demireller Mining company. The shale ore was systematically crushed for size reduction. The crushing process was carried out gradually with a Pulverisette I model (Fritsch) jaw crusher with adjustable outlet opening to a length of -4,75 mm, and one half of the crushed material was saved as witness sample. The other half was crushed further with a jaw crusher to -2 mm.

2.1. Characterization of the ore

X-ray diffraction (XRD) analyses were used to determine the mineral composition of Kızıldağ shale ore and intensively milled products, and to monitor the changes in the crystal properties of these minerals with milling. For this purpose, XRD patterns were obtained using a Rigaku MiniFlex 600 model XRD instrument (Munzur University) at CuKα (α: 1.5405 Å) irradiance, 2°/min scanning speed and diffraction angles ranging from 5-80º. A scanning electron microscope (SEM), Hitachi SU3500 model (Munzur University), was used to determine the micromorphological properties. BET surface area measurements were performed using a Micromeritics TriStar II Plus model surface area measuring system in a liquid nitrogen environment based on the N_2 gas adsorption technique. Perkin Elmer Elan 9000 model ICP-MS and ICP-AES instruments (ALS Labs) were used to determine the chemical content of the ore samples.

2.2. Milling of ore for mechanical activation

For mechanical activation, intensive-milling processes were carried out in a Fritsch Pulverisette 6 model mono-shaft planetary ball mill (İnönü University). The milling process was carried out in an air-cooled planetary ball mill with high energy efficiency, using a tungsten carbide mortar with an internal volume of 250 cm^3 and 10 mm diameter balls made of the same material as the mortar. The milling was carried out dry at milling speeds of 400 and 500 rpm, at ball-to-powder ratios (BPR) of 5, 10, and 20 by mass and for different durations ranging from 15 to 90 minutes.All samples were dried at 105 °C for at least 1 hour to remove surface moisture prior to milling and then cooled in a desiccator. To prevent overheating of the mill, the mill was programmed to run for 10 minutes followed by a 10 minute hold programme for cooling to complete the required milling time.

For evaluation of the milling intensity and planetary mill efficiency, the specific milling work or stress energy, SE ($J.kg^{-1}$) [19], was calculated using the Eq. 1.

$$SE\ (J.kg^{-1}) = (m_B/m_S) \cdot a \cdot n \cdot t_M \cdot D \qquad \text{(Eq. 1)}$$

where m_B, m_0, a, n, t_M and D refer to mass of milling media (kg), mass of material charge (kg), theoretical acceleration in the center of the bowl in the planetary mill (m/s^2), speed of the planetary mill (1/s), milling time (s) and inner mill diameter (m), respectively. Theoretical acceleration for the planetary ball mill is 26.41 m/s^2, as given by the supplier. With the help of data obtained by XRD analysis, crystalline state of the samples was calculated using Eq. 2. Effect of mechanical activation was evaluated by a mass fraction of the crystalline phase (X) in the milled sample. X was compared with the reference substance (unmilled substance) which is assumed to correspond to 100% crystalline [20]. Thus, it holds that,

$$\text{Degree of Crystallinity (X), \%} = (U_o I_x / I_o U_x) * 100 \qquad \text{(Eq. 2)}$$

where U_0 and U_X denote the backgrounds of unmilled (reference) sample and milled sample, while I_0 and I_X are integral intensities of diffraction lines of the mineral in the unmilled (reference) sample and milled sample, respectively. Accordingly, if $I_X = I_0$, it is interpreted that the mineral is 100% XRD crystalline or 0% XRD amorphous with respect to the diffraction surface (hkl) to which the peak belongs. The equation is based on the assumption that the mechanical activation is not accompanied by a texture error (e.g., due to preferential orientation where there was none in the unmilled sample). Complementary value of amorphization (A) (also called degree of amorphization or content of X-ray amorphous phase) can also be used. The degree of amorphization is found by subtracting 100 from the degree of crystallization (X).

3. Results and Discussion

3.1. Chemical properties

The chemical composition of bauxite-related shales is presented in Table 1 and Table 2. XRD analysis method was

used to determine the mineralogical content of Kızıldağ shale ore (Figure 1).

Table 1. Oxide content (%) of Kızıldağ shale ore determined by ICP-AES.

SiO_2	Al_2O_3	Fe_2O_3	CaO	MgO	Na_2O	K_2O	TiO_2	LOI
42.7	28.8	4.29	5.69	0.56	3.04	3.04	1.41	9.49

Table 2. REE content (ppm) of Kızıldağ shale ore determined by ICP-MS.

Ce	La	Y	Nd	Sc	Pr	Dy	Er	Gd	Sm
115.7	82.8	83.8	59.2	28	15.7	11.65	7.46	10.42	10.75
Yb	**Ho**	**Lu**	**Eu**	**Tb**	**Tm**	**∑REE**	**Rb**	**Th**	**U**
7.06	2.52	1.04	1.88	1.73	1.09	441.5	112	21.7	4.39

As a result of ICP-AES analysis in Table 1, Kızıldağ shale ore has an average content of 42.70% SiO_2 and 28.8% Al_2O_3. In the literature, it is stated that ionic clays contain approximately 500-3,000 ppm REE [15]. In Table 2, the total REE content was determined as 441.5 ppm, and it was found to have a low content compared to other studies on this deposit. Although it is low, it has the quality that can be evaluated within the limit grade. In the study conducted by Hepvidinli [15], it was stated that the REE content of Kızıldağ ore varies between 240-3,000 ppm. It is evaluated that this variability may be due to the formation of REE minerals such as allanite and serite in different regions of Kızıldağ region.

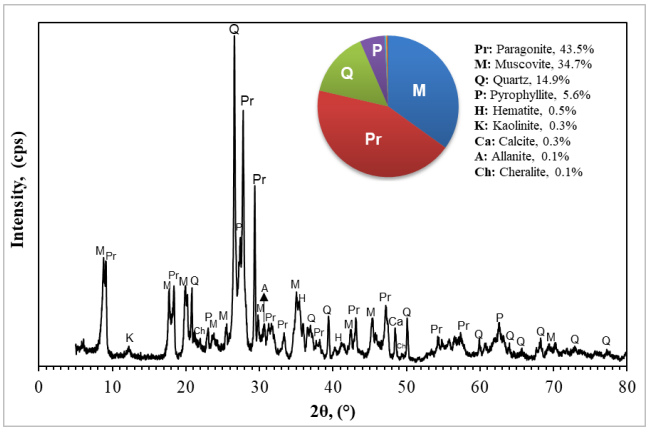

Figure 1. XRD pattern of Kızıldağ shale ore and its contents determined by Rietveld analysis (M: Muscovite, P: Pyrophyllite, Pr: Paragonite, Q: Quartz, K: Kaolinite, H: Hematite).

As analyzed by X-ray diffractometer (Fig. 1), the ore contains mainly paragonite ($NaAl_3Si_3O_{10}(OH)_2$, ICDD PDF# 24-1047), muscovite ($KAl_3Si_3O_{10})(OH)_2$; ICDD PDF# 07-0042), quartz (SiO_2; ICDD PDF# 46-1045), pyrophyllite ($Al_2Si_4O_{10}(OH)_2$; ICDD PDF# 46-1308), kaolinite ($Al_2Si_2O_5(OH)_4$; ICDD PDF# 29-1488), and hematite (Fe_2O_3; ICDD PDF# 80-5406).

3.2. XRD analysis of intensive-milled ore

XRD changes of the ore milled at 400 rpm mill speed, BPR: 10, 20 ratio and different milling times are given in Figure 2a-b. XRD patterns of the ore milled at 500 rpm mill speed for various times in Figure 3.

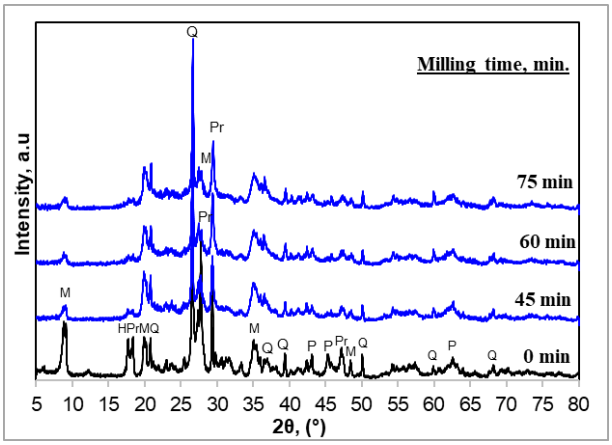

(a. BPR: 10)

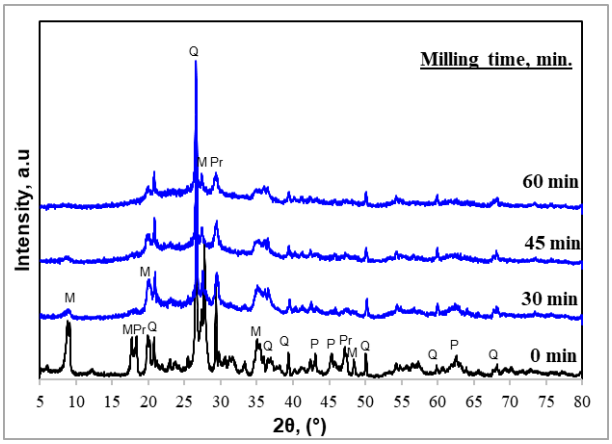

(b. BPR: 20)

Figure 2. XRD patterns of the ore milled at 400 rpm mill speed for various times (P: Pyrophyllite, Pr: Paragonite, M: Muscovite, C: Calcite, Q: Quartz).

Figure 2a shows that at all milling times, the peak intensities of profillite, paragonite and muscovite minerals slightly decreased compared to the unmilled sample. No significant change was observed with increasing milling time. Figure 2b shows the muscovite at 2θ: 9.52º decreased significantly at 30 and 45 minutes and disappeared completely at 60 minutes of milling time. The muscovite peak at 18,34º disappeared completely at 45 minutes of milling time. At 2θ: 35,06º, it is

observed that the peak broadens due to amorphization and the broadening increases as the milling time increases.

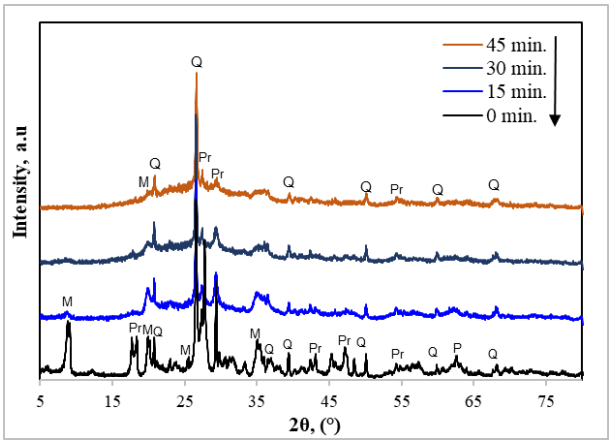

Figure 3. XRD patterns of the ore milled at 500 rpm mill speed for various times (Pr: Paragonite, M: Muscovite, Q: Quartz, P: Pyrophyllite, K: Kaolinite).

Upon examination of Fig. 3, it is evident that the peak intensities of the minerals decreased across all milling times. Only quartz, muscovite, and paragonite peaks remained discernible in the XRD pattern after 45 min of milling. Peaks associated with clay minerals such as pyrophyllite, paragonite, kaolinite, and halloysite were no longer detectable. Furthermore, it was observed that the muscovite peak at 2θ: 35.06° broadened because of amorphization, with the broadening increasing proportionally to the milling time. The peak intensities diminished more rapidly at 500 rpm milling speed compared to 400 rpm, indicating that mechanical activation was achieved in shorter durations at higher milling speeds. In addition, it is observed that the peaks disappear, and their intensity decreases in shorter periods at 500 rpm milling compared to 400 rpm milling speed. Thus, it is anticipated that activation can be realized in a shorter time at high milling speed.

Based on the XRD analysis data of the milled ores, the degree of amorphization of paragonite (2θ: 29.34°), quartz (2θ: 26.55°) and muscovite (2θ: 27.73°) in the ore was calculated. The variation of amorphization degrees of paragonite, muscovite and quartz minerals with milling time at a constant milling speed of 500 rpm and a constant ball to ore ratio of 20 is presented in Fig. 4.

It is seen that Fig. 4, in general, paragonite and muscovite have a high degree of amorphization while quartz has a significantly lower degree of amorphization. There is also an increasing trend in amorphization with milling time for all three minerals. It can also be seen that the amorphization degree of quartz is over 50% because of intensive milling. Considering the leaching efficiency, it is desirable that the quartz amorphized as little as possible to prevent the gelation of silica during the acid leaching.

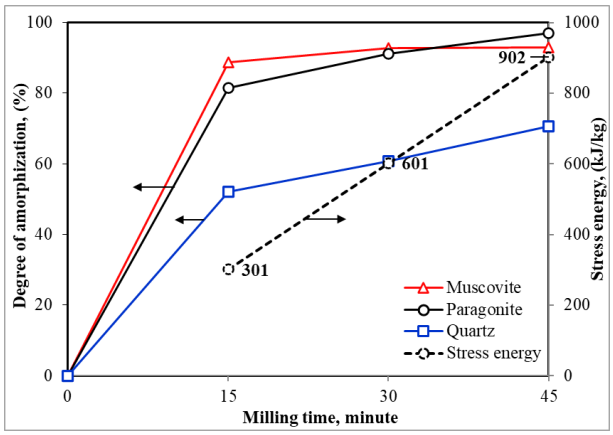

Figure 4. Variation of the degree of amorphization of paragonite, muscovite and quartz with milling time (500 rpm, BPR: 20).

3.3. SEM analysis of milled ore

The surface morphology of the intensive-milled products was examined with the help of SEM and the images obtained are given in Figure 5.

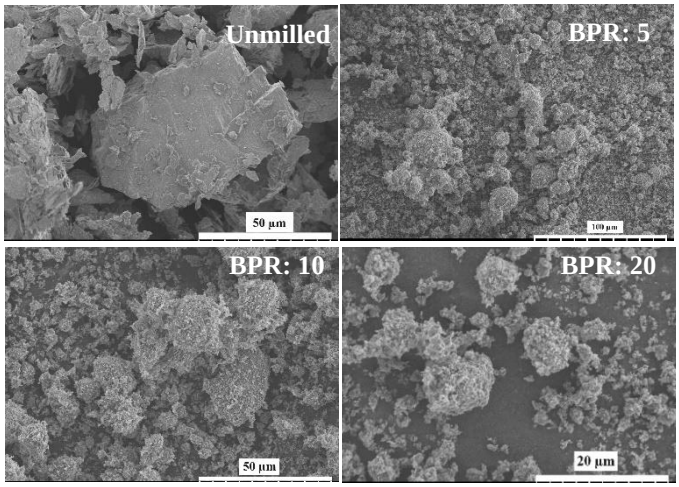

Figure 5. SEM images of unmilled and ore milled at 400 rpm, 45 min, BPR: 5-10-20 condition.

The layered/leaf-like structured particles shown in Fig. 5 unmilled ore considered clay minerals. The prismatic structured particle observed in Fig. 5 unmilled was also confirmed to be paragonite by XRD analysis. The spherical particles in Figure 5 400 rpm, 45 min, BPR: 5-10-20 condition are believed to be agglomerates comprising minerals with low hardness in the ore. In general, it was observed in SEM micrographs that the particle size of agglomerates decreased as the milling conditions became more severe. From the SEM microphotographs, it was seen that the particle sizes of the agglomerates decreased as the milling conditions became more intense.

3.4. BET surface area analysis

Surface area (SA) of unmilled and milled pyrophyllite samples were determined by BET surface area measurement based on nitrogen adsorption technique. Fig. 6 shows change of BET SA of milled shale with milling time.

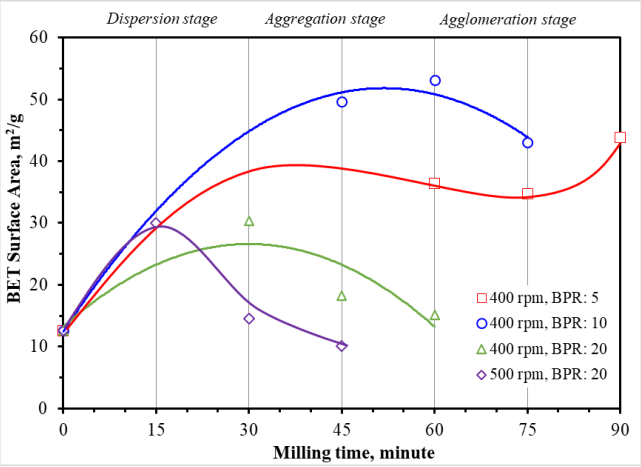

Figure 6. Change in BET specific surface area of shale ore milled at different BPR values and 400-500 rpm milling speed for different times.

According to the BET surface area analysis results, the ore is brittle and with milling the BET specific surface area increases from about 13 m^2/g to 55 m^2/g (Figure 6). As the milling time increases, an increase in BET surface area is observed in the dispersion phase and a general decrease is observed in the aggregation and agglomeration phases. During the aggregation and agglomeration phases, the surface area generally decreases due to the increase in agglomeration. At BPR: 5, an increase, then a decrease and again an increase is observed with increasing milling time. BPR: 10 is the milled product with the highest surface area compared to the others, and a parabolic increase was observed up to 60 minutes, and then a sharp decrease was observed in the agglomeration phase. It can be seen that the surface area of the shale ore increases up to 30 minutes at BPR: 20, but the surface area decreases after this period. BET specific surface area as a function of BPR except for BPR: 5, a decrease is observed after an increase up to a certain level. The reason for this is that the agglomeration effect of the ore particles occurs after a period of milling, as determined by SEM analysis of the milled ore.

3.5. TG analysis of intensively milled ore

Thermogravimetric analysis (TGA) curves of the ore samples milled at 400 rpm are shown in Figure 7 for different milling times (15-90 minutes) and compared. The maximum mass loss is around 6%, with a sharp decrease in the dehydroxylation zone between 470-750 °C, which is the most significant. This mass loss should be the indication of the disintegration of the hydrated structure, the occurrence of dehydration and dehydroxylation reactions, and the subsequent movement of interlayer water.

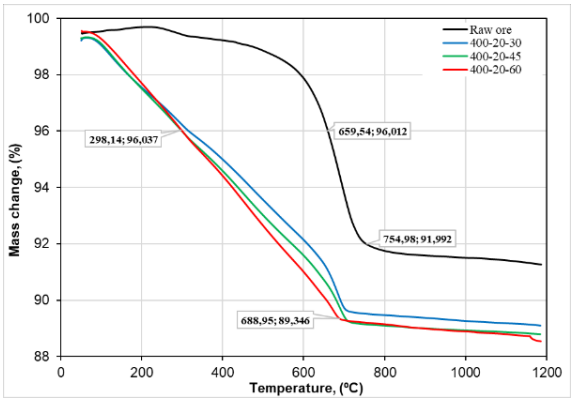

Figure 7. TGA curves of samples unmilled and milled at different times at 400 rpm mill speed.

The first notable finding in Figure 7 is that dehydroxylation, which is known to occur characteristically in the 550-800 °C temperature range in unmilled ores [21], starts at lower temperatures in milled ores. As milling time increases, mass loss increases. This is due to the formation of new surfaces and their influence by temperature. At 400 rpm, it was observed that the TGA curve shifted to the left due to the effect of intensive milling at all BPR, i.e. thermal changes occurred at lower temperatures.

It was also observed that the curves shifted more to the left up to BPR: 20 at a milling speed of 400 rpm. While the sharp point in the curve where mass loss decreases and dehydroxylation is largely complete was reached at 754.98 ºC with 8.01% mass loss in the raw ore, it was reached at 688.95 ºC with 10.65% mass loss in the intensive milled ore at 400-20-60 (rpm-BPR-time). In other words, at this point, a difference of 66.03 ºC and 2.64% occurred due to the effect of transformation (left shift) as a result of intensive milling. On the other hand, it can be seen that the mass loss after approximately 730 ºC as a result of milling for 45 minutes at a milling speed of 500 rpm at a ratio of BPR: 20 is even lower than that of the ore. While the mass loss of the fresh ore was 8.73%, the mass loss of the ore milled at 500-20-45 was 7.98%. This is due to the loss of water (dehydroxylation) in the crystalline structure in the mill during intensive milling.

4. Conclusion

In this study, shale ore containing mainly pyrophyllite, muscovite and quartz was mechanically activated by intensive milling to increase the leaching recovery. The effects of intensive milling on the structural properties of the ore and the thermal transformations during heating were investigated. In

general, pyrophyllite and muscovite were found to have a high degree of amorphization, whereas quartz had a significantly lower degree of amorphization. As a result of milling for 30 minutes, pyrophyllite and muscovite minerals were found to be over 80% amorphous, while quartz was 40% amorphous. SEM analysis showed that the particles were agglomerated, a typical result of intensive milling. According to the TG curves, dehydration and dehydroxylation occur at lower temperatures as BPR and milling speed increase, clearly showing the effect of mechanical activation. Based on all these results, it was concluded that the ore was mechanically activated. As a result, mechanically activated ore behaves more actively in the leaching process.

Declaration of Competing Interest

The authors declare that they have no known competing financial interests or personal relationships that could have appeared to influence the work reported in this paper.

Acknowledgement

The authors thank the Scientific and Technological Research Council of Turkey (TÜBİTAK) for financially supporting this study via Project No 122M810, Demireller Mining Inc. for providing shale ore samples from Ayrancı (Karaman, Turkey).

CRediT authorship contribution statement

Turan Uysal: Investigation, Validation, Formal analysis, Writing-original draft. ORCİD ID: 0000-0003-1643-6725

Tufan Kıyak: Investigation, Validation. ORCİD ID: 0000-0002-5438-3794

Hikmet Sis :Conceptualization, Writing-review & editing, Supervision. ORCİD ID: 0000-0001-8840-5448

Murat Erdemoğlu: Data curation, Writing-review & editing, Supervision. ORCİD ID: 0000-0003-2922-7965

References

[1] C.J., Warris, P.G., McCormick, Mechanochemical processing of refractory pyrite. Minerals Engineering, 10, (1997), 1119-1125.
[2] P., Baláž, Influence of solid state properties on ferric chloride leaching of mechanically activated galena. Hydrometallurgy, 40, (1996), 359-368.
[3] P., Baláž, Extractive Metallurgy of Activated Minerals, Amsterdam: Elsevier, (2000).
[4] T., Uysal, Investigation of activation conditions in alumina production from pyrophyllite ore by acid leaching method. PhD Thesis, Inonu University, Mining Engineering Department, (2018), Malatya, Türkiye.
[5] D., Tromans, J.A., Meech, Enhanced dissolution of minerals: microtopography and mechanical activation. Miner. Eng. 12, (1999), 609-625.
[6] N.J., Welham, Enhanced dissolution of tantalite/columbite following milling. Int. J. Miner. Process., 61, (2001), 145-154.
[7] N.J., Welham, Activation of the carbothermic reduction of manganese ore. Int. J. Miner. Process., 67, (2002), 187-198.
[8] M., Şener, T., Uysal, M. Erdemoğlu, Economic Evaluation of Thermal and Mechanical Activation Energies in Gypsum Production. Sci. Min. J., 63, (2024), Issue: 1, 47 - 52.
[9] B., Alyousif, T., Uysal, M.K., Aydemir, M. Erdemoğlu, Contribution of mechanical activation for obtaining potassium chloride from microcline. Min. Metall. Explor. 40, 4, (2023) 1311- 1319.
[10] M., Erdemoğlu, M., Birinci, T., Uysal, E., Porgalı, T.S., Barry, Acid leaching performance of mechanically activated pyrophyllite ore for Al_2O_3 extraction. J. Mater. Sci. 53, (2018), 13801-13812.
[11] N., Krishnamurthy, C. K. Gupta, Extractive Metallurgy of Rare Earths (Second Edition), (2016) CRC Press-Taylor & Francis Group.
[12] H., Öztürk, N., Hanilçi, S., Altuncu, C. Kasapçı, Rare earth element (REE) resources of Turkey: an overview of their characteristics and origin, Mineral Res. Expl. Bul., (2019) 159 143-129.
[13] E.C., Ünal, M., Karacahan, T., Uysal, Hydrometallurgical roadmaps and future strategies for recovery of rare earth elements. Miner. Process. Extr. Metall. Rev., (2023) https://doi.org/10.1080/08827508.2022.2073591.
[14] N., Hanilçi, Geological and geochemical evolution of the Bolkardağı bauxite deposits, Karaman, Turkey: Transformation from shale to bauxite. J. Geochem. Explor., (2013), 133, 118-137.
[15] B. Hepvidinli, Investigation of Rare Earth Element Contents of Kızıldağ and Kemiklitepe (Ayrancı-Karaman) Bauxite Mineralizations and Related Source Ores, M.Sc. Thesis, İstanbul Cerrahpaşa University, (2019), İstanbul, Turkey.
[16] T., Uysal, M.E., Akça, H., Sis, M., Erdemoğlu, Optimization of rare earth element recovery from Kızıldağ (Karaman-Türkiye) shale ore using response surface methodology. 18th International Mineral Processing Symposium, (2024), Eskişehir, Türkiye.
[17] T., Uysal, T., Kıyak, H., Sis, M., Erdemoğlu, Effect of intensive milling on the structural characteristics of shale ore. 22nd International Metallurgy and Materials Congress, (2024), İstanbul, Türkiye.
[18] M., Birinci, T., Uysal, M., Erdemoğlu, E., Porgalı, T.S., Barry, Acidic leaching of thermally activated pyrophyllite ore from Pütürge (Malatya-Türkiye) deposit. In: Proceedings of the 17th Balkan mineral processing congress, (2017), Antalya, Türkiye.
[19] P., Pourghahramani, E., Forssberg, Effects of mechanical activation on the reduction behavior of hematite concentrate. Int. J. Miner. Process., 82, (2007), 96-105.
[20] P. Baláž, Mechanochemistry in Nanoscience and Minerals Engineering. Berlin: Springer, (2008), p. 296.
[21] J., Schomburg, Thermal investigation of pyrophyllites, Thermochimica Acta, (1985), 93, 521-4.